Glycobiology vol. 19 no. 10 pp. 1136–1149, 2009
doi:10.1093/glycob/cwp113
Advance Access publication on August 11, 2009

Enabling techniques and strategic workflow for sulfoglycomics based on mass spectrometry mapping and sequencing of permethylated sulfated glycans

Shin-Yi Yu[2], Sz-Wei Wu[3], He-Hsuan Hsiao[3], and Kay-Hooi Khoo[1,2,3]

[2]Institute of Biochemical Sciences, National Taiwan University, Taipei 106, Taiwan; and [3]NRPGM Core Facilities for Proteomics and Glycomics, Institute of Biological Chemistry, Academia Sinica, Nankang, Taipei 115, Taiwan

Received on June 18, 2009; revised on July 17, 2009; accepted on July 18, 2009

Sulfate modifications on terminal epitopes of *N*- and *O*-glycans have increasingly been implicated as critical determinants mediating a diverse range of biological recognition functions. To address these low abundance but important sulfated glycans, and the sulfoglycome in general, further development of enrichment strategies and enabling mass spectrometry (MS)-based mapping techniques are needed. In this report, we demonstrate that the sulfated glycans, with and without additional sialylation, can be successfully permethylated by the sodium hydroxide slurry method and be distinguished from phosphorylated glycans by virtue of this derivatization. In conjunction with simple microscale post-derivatization fractionation steps, permethyl derivatives fully retaining the negatively charged sulfate moiety and separated from the nonsulfated ones, can be efficiently detected and sequenced de novo by advanced MS/MS in the positive-ion mode. In particular, we show that the highly sequence and linkage informative high energy collision induced dissociation (CID) MS/MS afforded by MALDI-TOF/TOF can be extended to sulfoglycomic applications. The sulfated parent ion selected for CID MS/MS was found to mostly retain the sulfate moiety and therefore allow efficient fragmentation via the usual array of glycosidic, cross ring, and concerted double cleavages. Collectively, the optimized strategy enables a high sensitivity detection and critical mapping of the sulfoglycome such as the one derived from lymph node tissues or cell lines in both negative and positive-ion modes. Novel sulfated epitopes were identified from a crude mouse lymph node preparation, which fully attested to the practical utility of the methodology developed.

Keywords: glycan sequencing/mass spectrometry/permethylation/sulfated glycans

Introduction

Mass spectrometry (MS) and various modes of separation techniques, coupled with chemical modifications and glycosidase digestions, are the corner stones of high sensitivity approach in structural determination of complex glycans derived from biological sources (Geyer H and Geyer R 2006; Morelle et al. 2006; Wuhrer et al. 2007). More recently, these glycosylation studies have evolved into what is referred to as glycomics, which involves mapping the complexity and characteristics of the glycome of a cell, tissue, or organism, at a particular physiological or genetically altered state (Haslam et al. 2006; Zaia 2008). From the onset, we and others have advocated high throughput and robust MALDI-based MS profiling and CID MS/MS sequencing of permethyl derivatives as the principal "first screen" strategy in glycomics (Jang-Lee et al. 2006; Yu et al. 2006; Wada et al. 2007). While the overall sequence, core type, and terminal epitope substituents were found to be best determined via low energy CID MS/MS due to its simplicity, high energy CID MS/MS on a TOF/TOF can provide valuable linkage information through additional cross-ring and other concerted cleavages, once a systematic assignment of the complicated cleavage pattern has been established (Hortin et al. 1986; Morelle et al. 2004; Spina et al. 2004; Stephens et al. 2004; Yu et al. 2006; Yu et al. 2008).

It is apparent that current limitations in MS/MS-based glycomic mapping lie not in detailed sequencing of the usual array of *N*- and *O*-glycans in isolation, but mostly in resolving complex isomeric mixtures and to detect glycans of low abundance, larger size with polyLacNAc chains, and/or those multiply substituted with negatively charged constituents. The sulfated glycome, in particular, is often refractory to MS-based glycomic mapping. Apart from the sulfated glycosaminoglycan on the proteoglycan, which merits its own systematic studies (Hitchcock et al. 2008; Zaia 2009), a most abundant source of mammalian-sulfated glycans is carried on the *O*-glycans of mucins lining the respiratory and gastrointestinal tracts, and the salivary mucins, which collectively provided a rich source of various sulfated epitopes for early MS-based structural studies and methodology development (Mawhinney et al. 1992; Lo-Guidice et al. 1994; Karlsson et al. 1996; Capon et al. 1997, 2001; Thomsson et al. 1999, 2000; 2005; Robbe et al. 2004). Other than that, most of the reported occurrences of sulfated *N*- and *O*-glycans (Hooper et al. 1996; Degroote et al. 1999; Gallego et al. 2001; Liedtke et al. 2001; Satomaa et al. 2002; Kanda et al. 2004) are based on radioisotope labeling with very few detailed structural studies being undertaken, which largely reflects a lack of sensitive analytical techniques including those based on MS. In cases where MS has been applied, mostly on purified, more abundant glycoproteins, analyses were often restricted to molecular weight determination without MS/MS to support the assigned glycosyl compositions (Kawasaki et al. 2001; Barboza et al. 2005; Murakami et al. 2007; Hernandez Mir et al. 2009).

[1]To whom correspondence should be addressed: E-mail: kkhoo@gate.sinica.edu.tw

Collectively, these works nonetheless revealed that the distribution of sulfated glycans and the structural diversity of the sulfated terminal glyco-epitopes are much wider than currently appreciated. Thus, whilst the 4-*O*-sulfated GalNAc unit on the terminal lacdiNAc element is rather restricted to the *N*-glycans of pituitary glycoprotein hormones (Green and Baenziger 1988), Gal-3-*O*-sulfate, Gal-6-*O*-sulfate, and GlcNAc-6-*O*-sulfate containing *N*- and *O*-glycans are widely distributed in mammalian lymphoid, central, and peripheral nerve tissues, inflammatory sites, and carcinomas. With increasing importance accorded to distinguishing the location of sulfation on sialyl Lewis A/X and sialyl LacNAc in relation to the specificities of the regulated expressed sulfotransferases (Hemmerich and Rosen 2000; Fukuda et al. 2001; McEver 2005; Kawashima 2006; Alon and Rosen 2007), it becomes more pressing than ever to develop and implement MS-based sulfoglycomic analyses that can resolve the structural differences better than that afforded by antibodies. These objectives require judicious choice of chemical derivatization and efficient front-end fractionation schemes with critical sample clean-up prior to MS analysis.

We reasoned that if sulfated glycans can likewise be efficiently permethylated, its mapping and sequencing will benefit from the kind of information rich low and high energy CID MS/MS in the positive-ion mode. This would rank superior to the commonly used ESI-MS/MS-based sequencing of the native sample from sulfated mucin (Thomsson et al. 2000, 2005; Robbe et al. 2004) in the negative-ion mode, which often do not give complete sets of linkage-specific cleavage ions. Further, without the *O*-Me tag, multiple cleavages are often indistinguishable from single cleavage and thus not conducive to definitive assignment of the branching pattern. Another critical consideration is that, unlike the abundant secretory mucous *O*-glycans, the low abundance of sulfated *N*- and *O*-glycans on the endothelial and myeloid cells would preclude high sensitivity direct detection by MS in the presence of biological matrix contaminants and the predominance of nonsulfated glycans. An advantage conferred by permethylation apart from facile clean-up is that selective detection can be effected in the negative-ion mode since only the sulfated glycans retain the negative charge whereas sialylated ones will be esterified (Mitoma et al. 2007). This strategy nevertheless does not extend to positive-mode MS/MS since the sulfated glycans are often not detectable in the sea of highly abundant neutral glycans when switched back to the positive-ion mode for them to be selected for MS/MS sequencing. Conversely, MS/MS performed in the negative-ion mode for the permethylated sulfated glycans, while being sensitive enough, did not afford sufficient discriminating cleavage ions that will unambiguously resolve isomeric sulfated structures.

We have therefore undertaken to optimize the permethylation protocols for the larger sulfated, sialylated complex-type *N*-glycan structures, as well as the smaller *O*-glycans, and developed an efficient microscale fractionation scheme to isolate the sulfated glycans away from the neutral ones. In the positive-ion mode, we now show that the sulfated glycans in general, and complex-type *N*-glycans in particular, can be effectively sequenced by high energy CID MS/MS on MALDI-TOF/TOF. Sulfate groups are fully retained and the fragmentation characteristics are similar to those already established for the nonsulfated glycans.

Results

MALDI-MS mapping and MS/MS sequencing of sulfated oligosaccharides

In comparison with the standard NaOH permethylation procedure commonly used to permethylate nonsulfated glycans, a critical step in ensuring a good recovery of the permethylated sulfated glycans is the passing of the quenched and neutralized reaction mixtures through C18 solid phase extraction (SPE) cartridge instead of direct partitioning against organic solvent such as chloroform. As demonstrated against a tetrasulfated diLacNAc tetrasaccharide, glycans with a charge density of up to 4 sulfate per 4 glycosyl residues could still be efficiently permethylated and eluted in the 25% acetonitrile fraction (Figure 1A). Excellent signal-to-noise ratio is attainable in the positive-ion mode when the starting material is at the low picomole level (Figure 1C) while the femtomole level detection sensitivity can be achieved if the permethylated sample is further diluted.

In general, sodiated molecular ions were observed with the number of sodium counter cations corresponding to the number of sulfate groups carried plus one extra to give it an overall single positive charge. Thus, a fully methylated tetrasulfated diLacNAc afforded a penta-sodiated molecular ion, $[M + 5Na–4H]^+$, at *m/z* 1319 (Figure 1A). An advantage of analyzing the permethylated glycan, compared with analysis of underivatized sample, is that it allows molecular ions carrying lower degrees of sulfation to be distinguished from fragment ions generated in the source through successive neutral losses of sodium sulfites (minus 102 u). On this basis, it can be concluded from the MALDI-MS data that, under the optimized experimental conditions, no desulfation was induced since molecular ions corresponding to tri-, di-, and monosulfated diLacNAc were not detected. In contrast, di- and monosulfated diLacNAc generated by partial methanolysis prior to permethylation did indeed afford $[M + 3Na–2H]^+$ and $[M + 2Na–H]^+$ molecular ions at *m/z* 1143 and 1055, respectively (Figure 1B), each accompanied by further neutral losses of sodium sulfites.

To obtain sequence information, either the intact molecular ions or those derived from neutral loss of sodium sulfite can be selected for MS/MS analysis. It is of interest to note that although neutral loss of sodium sulfite occurs readily during MALDI-MS analysis through in source prompt fragmentation, it is not a preferred cleavage mode when the sulfated molecular ions are subjected to CID MS/MS in the positive-ion mode. Loss of sulfate appears to occur more readily in ion trap for ESI-MS/MS of parents of higher charge state (data not shown) via elimination (minus 120 u) but minimal under MALDI-MS/MS on a Q/TOF or TOF/TOF. In fact, as shown for the monosulfated derivatives (Figure 2), the high energy CID fragmentation pattern observed resembles that afforded by nonsulfated, permethylated glycans, which have been studied extensively (Morelle et al. 2004; Stephens et al. 2004; Yu et al. 2006, 2008). In other words, the presence of an additional sulfate moiety does not significantly alter the established MS/MS cleavage pattern. Unambiguous assignment of the sulfated residue and the overall glycan structure can therefore be readily achieved based on the usual range of sequence informative and/or linkage-specific fragment ions.

MS/MS data interpretation is, however, more complicated when the parent ion in question is a composite of several

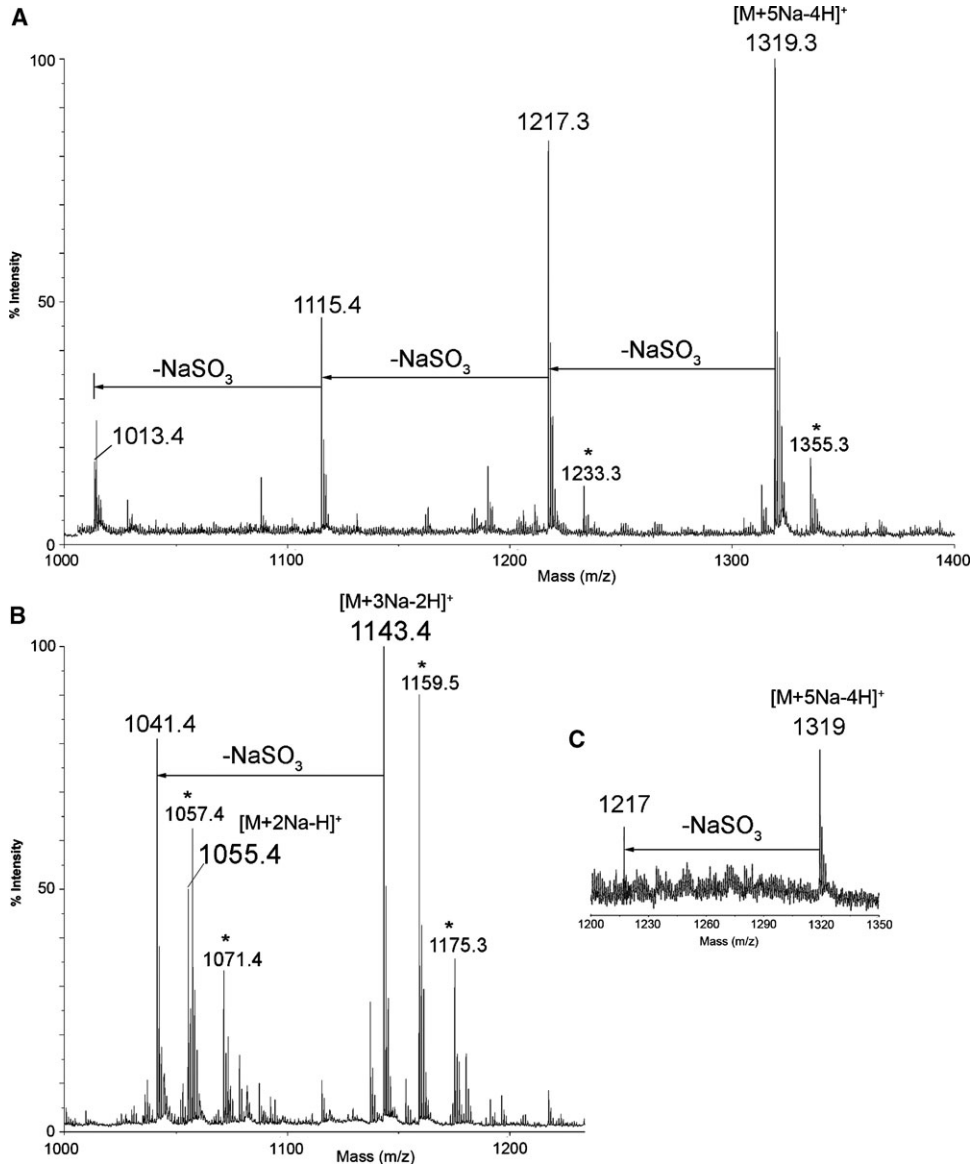

Fig. 1. MALDI-MS profiles of permethylated sulfated diLacNAc in the positive-ion mode. A tetrasulfated diLacNAc oligosaccharide standard (1 nmole) was permethylated either directly (**A**) or after partial desulfation to di- and monosulfated oligosaccharides by methanolysis (**B**). 1/40th of the 25% acetonitrile eluate from the C18 Sep-Pak cartridge was spotted onto the target plate to give the MALDI-MS spectra shown. As little as 50 pmole of starting material can be permethylated efficiently to give a molecular ion of a sufficiently good S/N ratio, as shown in (**C**), when 1/20th (equivalent to 2.5 pmole or less) of the recovered tetrasulfated permethyl derivatives was spotted for MALDI-MS analysis. Sodiated molecular ions were denoted as $[M+nNa-(n-1)H]^+$, which can be distinguished from successive neutral losses of sodium sulfite moieties (net loss of 102 u after gaining a proton, annotated as -$NaSO_3$), as indicated. Each substitution of the sodium counter cation by a potassium gives additional satellite signals at 16 u higher, denoted by an asterisk.

isomeric forms, as often encountered in biological samples. The monosulfated diLacNAc derived from methanolysis of a tetrasulfated diLacNAc standard (Figure 1) is expected to comprise isomers with the single sulfate possibly retained on any of the four glycosyl residues, thus exemplifying a naturally occurring heterogeneity. As shown in Figure 2A for the high energy CID MS/MS spectrum of this molecular ion species ($[M+2Na–H]^+$ at *m/z* 1055), the dominant cleavages were directed to the internal GlcNAc, as expected for a Gal-GlcNAc-Gal-GlcNAc backbone structure, producing abundant B and Y ion pairs. B ions at *m/z* 486 and 574, which pair with the Y ions at *m/z* 592 and 504, respectively, indicate that the sulfate can be located on either of the two LacNAc units (isomeric structures I and II). Additional ^{1,5}X and G ions at *m/z* 865 and 789 show that the nonreducing terminal Gal is mostly not sulfated, thus placing the sulfate on the internal GlcNAc for isomer II that carries the sulfate on the nonreducing-end LacNAc unit. This is further supported by the D ion at *m/z* 560, derived from cleavages at the internal GlcNAc. On the other hand, the ^{1,5}X ion at *m/z* 416 and G ion at *m/z* 340 implicate a sulfated reducing-end GlcNAc for isomer I, whereas the possible presence of sulfate on the internal Gal is indicated by the D ion at *m/z* 315. Thus, the sulfate may be carried on either the Gal or GlcNAc of the reducing terminal LacNAc unit. Other ions can be assigned accordingly as schematically illustrated (Figure 2A).

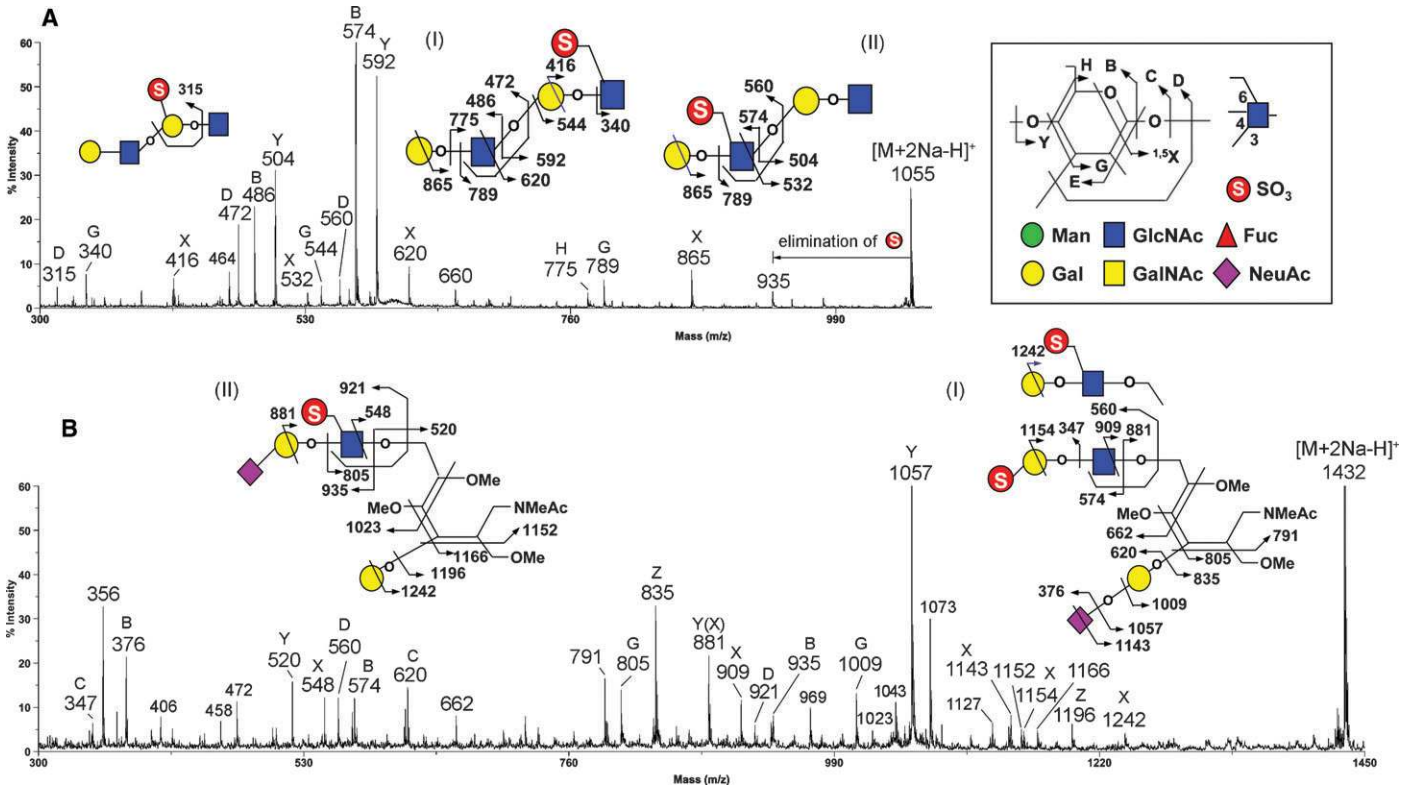

Fig. 2. High energy CID MALDI-MS/MS fragmentation characteristics of permethylated sulfated glycans in the positive-ion mode. Representative high energy CID MS/MS spectra for the permethylated monosulfated diLacNAc derived from partial methanolysates of a tetrasulfated diLacNAc oligosaccharide standard (**A**) and a sialylated sulfated core 2 *O*-glycan from human ovary cyst mucin (HOC350) (**B**) are shown here along with schematic drawings of the deduced isomeric structures to illustrate the assignment of the major fragment ions. Key symbols and the fragment ion nomenclature used (Yu et al. 2006, 2008) are shown in the boxed inset. For simplicity, peaks corresponding to ^{1,5}X ions are labeled as X without the superscript. In addition to the sequence informative B, Y, ^{1,5}X, G and D ions described in the text, NeuAcα2,3-sialylation typically gives an ion at *m/z* 356 in addition to the oxonium ion at *m/z* 376, corresponding to a sodiated C_1 ion having eliminated the COOMe moiety (Lemoine et al. 1993). Loss of NeuAc additionally gave a characteristic doublet of 2 mass units apart corresponding to ^{1,5}X and ^{O,2}X ion, usually further accompanied by another signal doublet at 16 mass units lower (*m/z* 1143/1141 and 1127/1125). Notably, the G ion at *m/z* 1009 indicates that NeuAc is carried on the C3 of Gal (in Figure 2B), consistent with the prominent ion observed at *m/z* 356. For structure I in (**B**), no critical ion can positively identify the alternative location of sulfate on the GlcNAc, nor ruling it out, due to coexistence of isomers that share common fragment ions. The position of sulfate on the Gal was not established by this study.

As a second representative case example, MS/MS analysis on a typical mucin-type sialylated sulfated core 2 *O*-glycan demonstrated that sialylated sulfated glycan can likewise be fully methylated and analyzed in the positive-ion mode, giving rise to the same array of sequence-informative fragment ions. The major isomers identified are structures with either a sulfated LacNAc or sialylated sulfated LacNAc on the 6-arm, as supported by the respective B (*m/z* 574, 935), Y (*m/z* 881, 520), ^{1,5}X (*m/z* 909, 548), D (*m/z* 560, 921), and the Z_1 (*m/z* 835, 1196) ions (Figure 2B, see assignment on isomeric structures I and II). The presence of a terminal sulfated Gal among the isomers is clearly indicated by the ^{1,5}X ion at *m/z* 1154 and the C ion at *m/z* 347. However, the MS/MS data itself cannot establish if the sulfate moiety may also be carried on the GlcNAc of sulfated LacNAc in structure I since the discriminating fragment ion at *m/z* 1242 can also be afforded by structure II. Such a limitation is often encountered in glycomic analysis of nonpurified glycan entities. In this context, a better MS/MS capability provided by the positive-ion mode analysis of the permethyl derivatives will facilitate detection of a full complement of existing structural isomers. It was noted that the abundant B and Y ion pairs, which are useful to localize the sulfate moiety to a particular LacNAc unit, are also the major fragment ions afforded by sodiated parents under low energy CID MS/MS as performed on a Q/TOF (data not shown). However, only high energy CID MS/MS on a TOF/TOF additionally gives the cross ring and satellite ions that allow distinguishing location of sulfate on either the Gal or GlcNAc of the LacNAc and additionally confirms the overall sequence and linkage of the glycan carrier. In particular, the relatively abundant D ions resulting from concerted double cleavages (Yu et al. 2006, 2008) are very useful to detect the presence of the internal sulfated Gal or GlcNAc residue in the context of a further substituted sulfated LacNAc unit.

Fractionation and MALDI-MS mapping of the sulfated N-glycans

Having established the efficiency of permethylating sulfated glycans and their salient features under MALDI-MS and MS/MS, focus was then turned to analyzing sulfated complex-type *N*-glycans of larger size. *N*-Glycans derived from recombinant erythropoietin (rEPO) produced in baby hamster kidney 21 (BHK21) cell line have been reported to contain sulfated components (Kawasaki et al. 2001). Following a simple C18 SPE fractionation, MALDI-MS analyses in the positive-ion mode indicated that the permethylated sulfated *N*-glycans were mostly eluted in the 25% acetonitrile fraction (Figure 3A). The

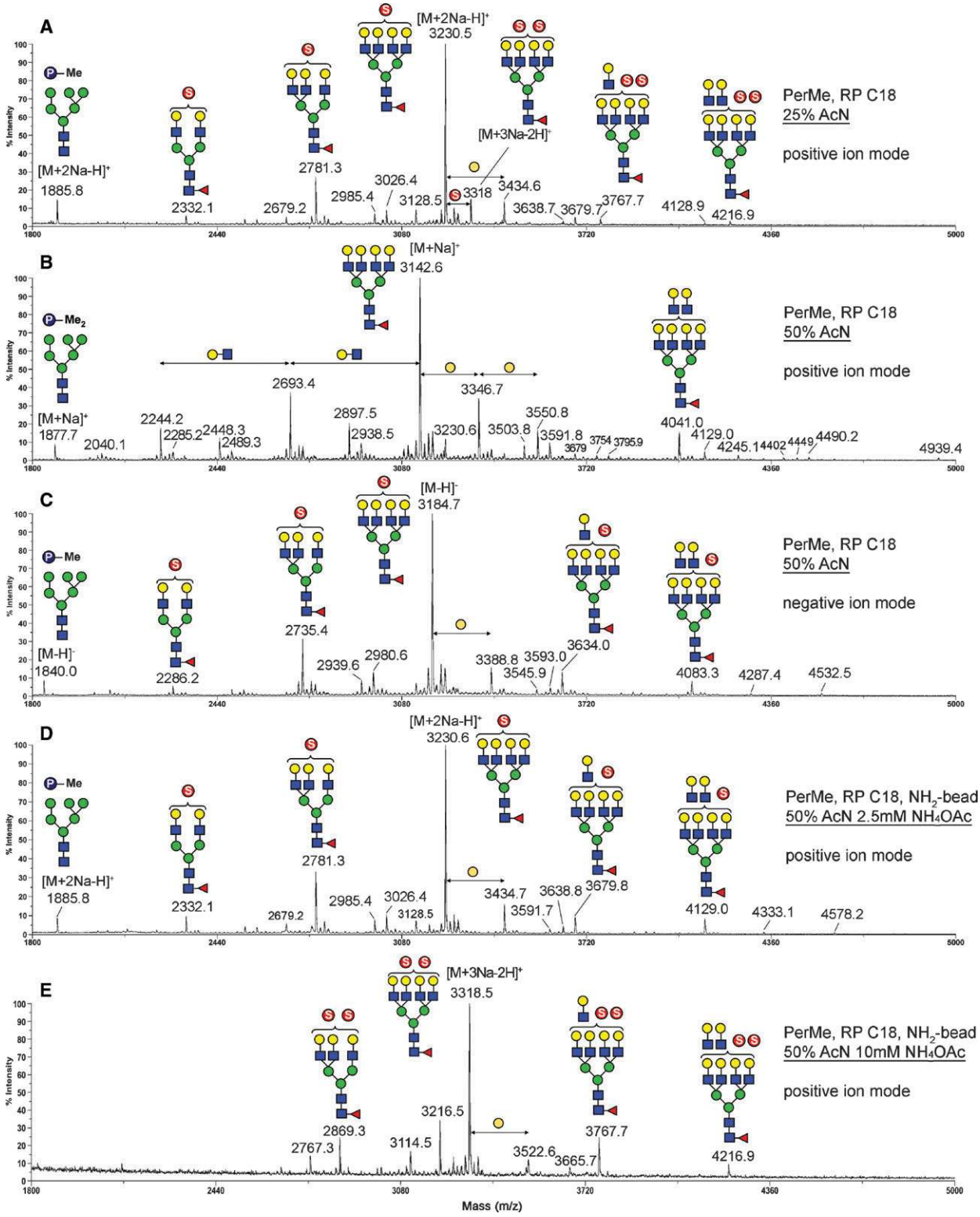

Fig. 3. MALDI-MS profiles of permethylated *N*-glycans from rEPO in positive- and negative-ion modes after various modes of fractionation. Permethylated sample was directly fractionated on C18 Sep-Pak cartridge and step-wise eluted with 25% (**A**) and 50% acetonitrile (**B**, **C**), with both fractions screened by MALDI-MS in both positive-(**A**, **B**) and negative-ion modes (**C**, and data not shown for the 25% acetonitrile fraction), using DHB and DABP as matrices, respectively. Either the pooled or individual 25% and 50% acetonitrile fractions from C18 Sep-Pak could be further subjected to fractionation on NH_2-beads. Monosulfated and disulfated glycans were found to be mostly eluted by 2.5 mM (**D**) and 10 mM (**E**) ammonium acetate in 50% acetonitrile, respectively, and detected in the positive-ion mode (**D**, **E**), free from suppression of the neutral glycans, which were eluted in the wash fraction (data not shown). In the positive-ion mode, signals at 102 u lower than the assigned molecular ions of sulfated glycans (see Table I) correspond to neutral loss of a sodium sulfite moiety due to in source prompt fragmentation.

Table I. Assignment of the molecular ion signals afforded by MALDI-MS mapping of the permethylated *N*-glycans released from rEPO glycoprotein. All detected major molecular ion signals in both positive- and negative-ion modes after various fractionation steps (Figure 3) were compiled together, except those attributed to the phosphorylated $Hex_6HexNAc_2$. Symbols used: C, trimannosyl core, $Hex_3HexNAc_2$; CF, fucosylated core; N, HexNAc; H, Hex; (HN), LacNAc unit; F, Fuc

Di-sulfated glycans			Nonsulfated glycans	
$[M+3Na-2H]^+$		Deduced composition	$[M+Na]^+$	Deduced composition
2869.2		$Na^+(SO_3^-)_2(HN)_3$ CF	2040.1	$N_1(HN)_1$ CF
3318.4		$Na^+(SO_3^-)_2(HN)_4$ CF	2244.2	$(HN)_2$ CF
3522.5		$Na^+(SO_3^-)_2H_1(HN)_4$ CF	2285.2	$N_2(HN)_1$ CF
3767.7		$Na^+(SO_3^-)_2(HN)_5$ CF	2448.3	$H_1(HN)_2$ CF
4216.9		$Na^+(SO_3^-)_2(HN)_6$ CF	2489.3	$N_1(HN)_2$ CF
			2693.4	$(HN)_3$ CF
Mono-sulfated glycans			2897.5	$H_1(HN)_3$ CF
$[M+2Na-H]^+$	$[M-H]^-$	Deduced composition	2938.5	$N_1(HN)_3$ CF
2332.1	2286.2	$SO_3^-(HN)_2$ CF	3142.6	$(HN)_4$ CF
2781.3	2735.4	$SO_3^-(HN)_3$ CF	3346.7	$H_1(HN)_4$ CF
2985.4	2939.6	$SO_3^-H_1(HN)_3$ CF	3503.8	$NeuAc_1(HN)_4$ CF
3026.4	2980.6	$SO_3^-N_1(HN)_3$ CF	3550.8	$H_2(HN)_4$ CF
3230.5	3184.7	$SO_3^-(HN)_4$ CF	3591.8	$(HN)_5$ CF
3434.6	3388.8	$SO_3^-H_1(HN)_4$ CF	3754.9	$H_3(HN)_4$ CF
3591.7	3545.9	SO_3^-Neu $Ac_1(HN)_4$ CF	3795.9	$H_1(HN)_5$ CF
3638.7	3593.0	$SO_3^-H_2(HN)_4$ CF	4041.0	$(HN)_6$ CF
3679.7	3634.0	$SO_3^-(HN)_5$ CF	4245.1	$H_1(HN)_6$ CF
4129.0	4083.3	$SO_3^-(HN)_6$ CF	4402.2	$NeuAc_1(HN)_6$ CF
4333.1	4287.4	$SO_3^-H_1(HN)_6$ CF	4449.2	$H_2(HN)_6$ CF
4578.2	4532.5	$SO_3^-(HN)_7$ CF	4490.2	$(HN)_7$ CF
			4939.4	$(HN)_8$ CF

disodiated molecular ion signals detected could be assigned as monosulfated, core fucosylated bi-, tri-, and tetra-antennary complex-type *N*-glycans, with and without further LacNAc unit increment and/or α-Gal modification (Table I). Additional signals corresponding to disulfated complex-type *N*-glycans were also detected at *m/z* 3318, 3767, and 4216. In contrast, the 50% acetonitrile fraction afforded mostly positive-ion signals corresponding to the nonsulfated, neutral, and sialylated *N*-glycans (Figure 3B, Table I).

Interestingly, it was observed that a phosphorylated $Hex_6HexNAc_2$ could either be mono- or di-*O*-methyl-esterified on the phosphate group (confirmed by MS/MS analysis, data not shown), thus retaining a negative charge or being neutralized, respectively. The two species were separated accordingly into the 25% and 50% acetonitrile fractions, giving rise to the detected $[M+2Na-H]^+$ signal at *m/z* 1885 and $[M+Na]^+$ signal at *m/z* 1877, respectively, in the positive-ion mode. However, when switched to the negative-ion mode, the MALDI-MS profile showed that the 50% acetonitrile fraction also contained the negatively charged mono-*O*-methyl-esterified species, which was preferentially detected as $[M-H]^-$ at *m/z* 1840. More importantly, most of the monosulfated *N*-glycans were in fact found to be eluted not only in the 25% but also the 50% acetonitrile fraction (Figure 3C). The highly abundant neutral *N*-glycans coeluted in the 50% acetonitrile fraction have rendered these negatively charged monosulfated *N*-glycans cryptic in the positive-ion mode, most likely due to ion suppression. Further fractionation is therefore needed to isolate the permethylated sulfated *N*-glycans away from the neutral ones to facilitate their detection.

For this purpose, an amine-based stationary phase fractionation was adapted for microscale applications, taking advantage of its weak anion exchange property. The C18 Sep-Pak 50% acetonitrile fraction described above, which contained monosulfated, neutral, and sialylated *N*-glycans, was loaded onto a micropipette tip packed with amine (NH_2-) beads and eluted with increasing concentration of ammonium acetates in 50% acetonitrile. MALDI-MS screening showed that the noncharged permethylated *N*-glycans, both neutral and sialylated ones, were recovered in the unbound and 95% acetonitrile wash fractions (data not shown), whereas the permethylated monosulfated *N*-glycans were eluted by 50% acetonitrile containing 2.5 mM ammonium acetate, along with the mono-*O*-methyl-esterified phosphorylated glycan (Figure 3D). For the C18 Sep-Pak 25% acetonitrile fraction similarly fractionated on the NH_2-beads micro-column, the permethylated monosulfated *N*-glycans were likewise eluted by 50% acetonitrile containing 2.5 mM ammonium acetate, whereas the permethylated disulfated *N*-glycans were eluted by 50% acetonitrile containing 10 mM ammonium acetate (Figure 3E). This two-step elution thus proved to be rather efficient in fractionating mono- and disulfated *N*-glycans.

Since the initial fractionation of the permethylated *N*-glycans on C18 Sep-Pak would inevitably lead to the variable degree of partitioning the monosulfated *N*-glycans into both 25% and 50% acetonitrile fractions, an alternative strategy is to use the initial C18 Sep-Pak step simply to clean-up the permethyl derivatives from the methylating reagents/solvents without fractionation. MALDI-MS screening in the negative-ion mode will reveal if sulfated *N*-glycans may be present and if so detected, the sample can be subjected to amine-based weak anion exchange for fractionation into neutral, monosulfated, and disulfated *N*-glycans. Such a fractionation scheme was indeed proven to be successful using the same sample derived from EPO as above. An added advantage is that the usually much less abundant

disulfated complex-type *N*-glycans could be efficiently enriched in a fraction (Figure 3E) separated from the monosulfated *N*-glycans (Figure 3D). This allows their better detection and selection for MS/MS, in comparison with the profile obtained without additional fractionation (Figure 3A).

MALDI-MS/MS of sulfated N-glycans

Judicious choice of fractionation scheme would increase the depth of any glycomic mapping as discussed above. All MS signals detected above a certain intensity threshold can then be selected for MS/MS analysis. As demonstrated with the smaller sulfated oligosaccharides (Figure 2), we further determined that permethylated sulfated *N*-glycans likewise fragment accordingly under high energy CID MS/MS in the positive-ion mode. The usual array of glycosidic cleavages B and Y ions, cross ring cleavages A and X ions, and concerted elimination of glycosyl substituents around the ring (E, G, H ions), as well as the characteristic D and C″/Y ions noted previously (Harvey et al. 1997; Stephens et al. 2004; Yu et al. 2006; Chen et al. 2008; Suzuki et al. 2009), collectively enable a highly informative sequence and linkage assignment of the implicated sulfated *N*-glycan structures, as illustrated in the respective figures.

Among the most critical MS/MS, fragment ions identified for the permethylated mono- and disulfated tetra-antennary *N*-glycans from rEPO (Figure 4) are as follows:

(i) A complementary series of reducing-end (^{1,5}X, Y, G, H) and nonreducing-end (B, E, D, ^{3,5}A) fragment ions that firmly establish the sequence of the terminal sulfated and nonsulfated LacNAc units.
(ii) Y_1 ion at *m/z* 474, which positively identifies core fucosylation, with no other B, ^{1,5}X or Y ions indicative of the additional presence of fucosylated terminal epitopes apart from LacNAc and sulfated LacNAc.
(iii) $^{1,5}X_3$ ions at *m/z* 2054/2142 (for monosulfated structure) and *m/z* 2054/2142/2230 (for disulfated structure), together with the D ions formed at the β-Man to give the signals at *m/z* 1329 and 1417, which collectively define the overall substituents on either of the two arms of the 3,6-linked β-Man. As illustrated in Figure 4, these ions are indicative of the presence of isomers in which the single sulfate in the mono-sulfated *N*-glycans can be distributed to either of the two arms. In the case of disulfated *N*-glycans, the two sulfates can either be both on the 3-arm or one distributed to either arm but not both on the 6-arm.
(iv) C″/Y ions at *m/z* 692 for the monosulfated structures and *m/z* 692 and 780 for the disulfated structures. The latter indicates that the additional sulfate moiety can be carried on the LacNAc antennae 4- or 6-linked to α-Man, whereas the single sulfate is preferentially located on the LacNAc antennae 2-linked to the α-Man.

Fractionation and analysis of sulfated O-glycans

Although the mucin-type *O*-glycans from some sample sources can be highly extended to a size comparable to *N*-glycans, a substantial proportion of the sulfated *O*-glycans are expected to be of smaller sizes and may behave differently under the fractionation scheme developed. To verify the general applicability of the C18 and NH_2-based fractionations to both permethylated *N*- and *O*-glycans in sulfo-glycomic mapping, *O*-glycans were derived from a crude preparation of mouse secondary lymph nodes for MS analysis. As in the treatment of the released *N*-glycans (Mitoma et al. 2007), the *O*-glycans additionally released from the de-*N*-glycosylated sample by alkaline reductive elimination were permethylated and directly fractionated on C18 Sep-Pak cartridge into 25% and 50% acetonitrile fractions. It was found that most of the nonsulfated *O*-glycans were indeed detected in the 50% acetonitrile fraction but, unlike the *N*-glycans, a significant amount of the smaller nonsulfated ones was also eluted in the 25% acetonitrile fraction. Importantly, MALDI-MS screening in the negative-ion mode (data not shown) indicated that the sulfated *O*-glycans were mostly contained within the 25% acetonitrile fraction but were either nondetected or similar in mass to other nonsulfated ones in the positive-ion mode (data not shown but similar to Figure 5A). This fraction was thus subjected to an additional NH_2-based fractionation step to isolate the sulfated permethylated *O*-glycans.

Table II. Assignment of the molecular ion signals afforded by MALDI-MS mapping of the permethylated *O*-glycans released from mouse secondary lymph nodes. Only the major signals detected within the mass range of *m/z* 800–2000 for the C18 Sep-Pak 25% acetonitrile fraction are listed, corresponding to the mass region of the spectra shown in Figure 5A and B for nonsulfated and sulfated *O*-glycans, respectively. Higher molecular weight components were additionally detected at above *m/z* 2000, as well as in the C18 Sep-Pak 50% acetonitrile fraction

Monosulfated glycans		Nonsulfated glycans	
$[M+2Na-H]^+$	Deduced composition	$[M+Na]^+$	Deduced composition
1071.5	$SO_3^-H_2N_2$-itol	895.5	$NeuAc_1$-H_1N_1-itol
1112.5	$SO_3^-H_1N_3$-itol	925.5	$NeuGc_1$-H_1N_1-itol
1245.6	$SO_3^-F_1H_2N_2$-itol	983.5	H_2N_2-itol
1316.6	$SO_3^-H_2N_3$-itol	1024.5	H_1N_3-itol
1432.7	$SO_3^-NeuAc_1H_2N_2$-itol	1140.6	$NeuAc_1$-H_1N_2-itol
1473.7	$SO_3^-NeuAc_1H_1N_3$-itol	1157.6	$F_1H_2N_2$-itol
1490.7	$SO_3^-F_1H_2N_3$-itol	1187.6	H_3N_2-itol
1520.7	$SO_3^-H_3N_3$-itol	1228.6	H_2N_3-itol
1677.8	$SO_3^-NeuAc_1H_2N_3$-itol	1256.6	$NeuAc_2H_1N_1$-itol
1765.9	$SO_3^-H_3N_4$-itol	1286.6	$NeuAc_1NeuGc_1H_1N_1$-itol
1922.9	$SO_3^-NeuAc_1H_2N_4$-itol	1316.7	$NeuGc_2H_1N_1$-itol
1970.0	$SO_3^-H_4N_4$-itol	1344.7	$NeuAc_1H_2N_2$-itol
		1374.7	$NeuGc_1H_2N_2$-itol
		1385.7	$NeuAc_1H_1N_3$-itol
		1432.7	H_3N_3-itol
		1473.8	H_2N_4-itol
		1589.8	$NeuAc_1H_2N_3$-itol
		1677.9	H_3N_4-itol
		1763.9	$NeuAc_1F_1H_2N_3$-itol

A significantly distinct positive-ion mode MALDI-MS profile was afforded by the 50% acetonitrile containing 2.5 mM ammonium acetate-eluted fraction (Figure 5B) in comparison with the unbound fraction (Figure 5A), which is almost indistinguishable from the original C18 Sep-Pak 25% acetonitrile fraction except for the absence of a peak at *m/z* 1071 in the latter, assigned as a sulfated core 2 *O*-glycan. In fact, additional MALDI-MS screening in the negative-ion mode and MS/MS analyses in the positive-ion mode showed that all major peaks found in the unbound and eluted fractions are nonsulfated and sulfated *O*-glycans, respectively (Table II), including the common signals at *m/z* 1316 and 1677. The former (*m/z* 1316) was identified by MS/MS as $[M+Na]^+$ of $NeuGc_2Hex_1HexNAc$-itol in the unbound fraction but as sulfated $Hex_2HexNAc_3$-itol in the eluted fraction (see annotated structures in Figure 5A and B).

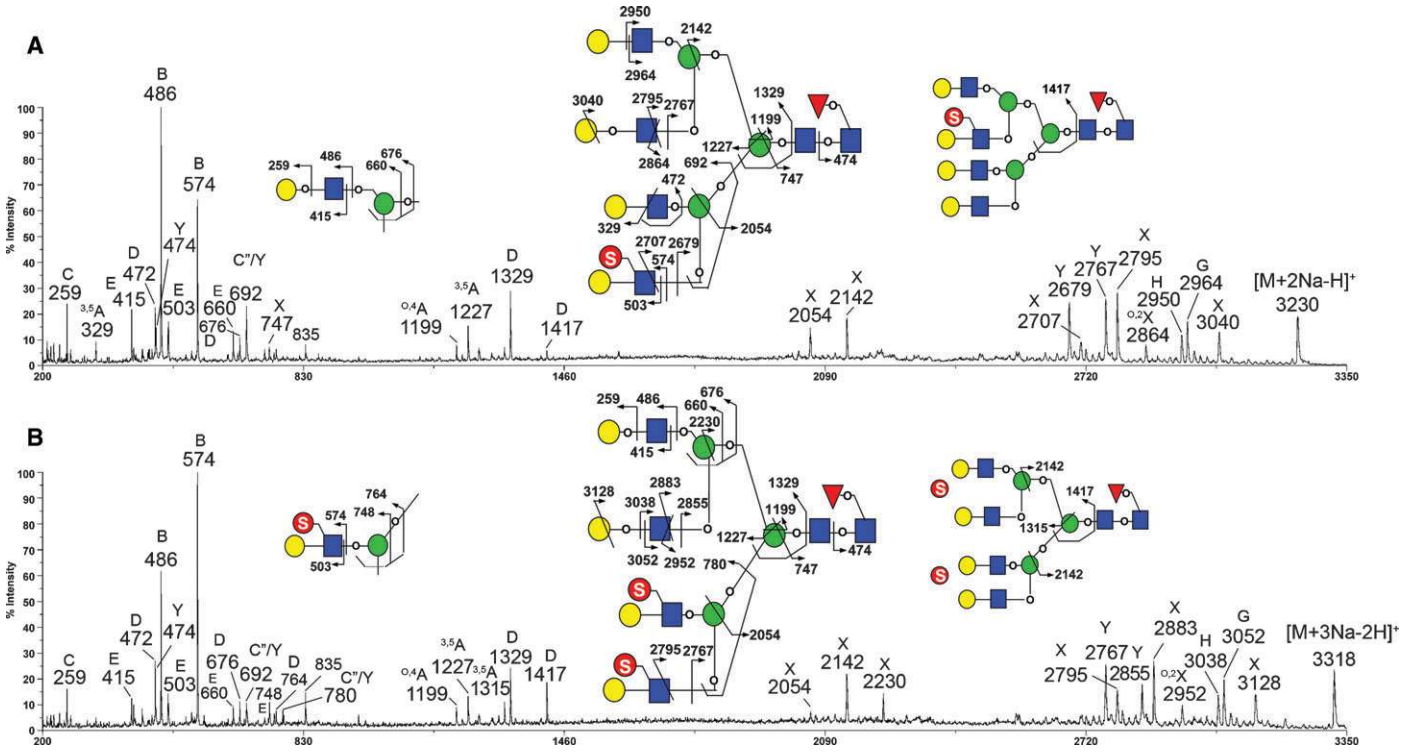

Fig. 4. MALDI-MS/MS sequencing of the permethylated sulfated *N*-glycans from rEPO in the positive-ion mode. Representative high energy CID MS/MS spectra acquired with MALDI-TOF/TOF are shown for $[M+2Na–H]^+$ of a mono-sulfated $Fuc_1Hex_7HexNAc_6$ at *m/z* 3230 (**A**) and $[M+3Na–2H]^+$ of a disulfated $Fuc_1Hex_7HexNAc_6$ at *m/z* 3318 (**B**). Sulfated and non-sulfated LacNAc terminal epitopes are primarily defined by the B ions at *m/z* 574 and 486, respectively, and further corroborated by the corresponding E, Y, and ^{1,5}X ions. The G and H ion pairs resulting from eliminating the terminal Gal are supportive of a Gal-4GlcNAc linkage of the LacNAc unit. Full assignments of the fragment ions are illustrated with drawings showing the coexisting isomeric structures and the ion types of the assigned signals were annotated accordingly. Key symbols are as defined in Figure 2.

The latter (*m/z* 1677) was likewise identified as nonsulfated $Hex_3HexNAc_4$-itol in the unbound fraction (Figure 5C) but sulfated $NeuAc_1HexNAc_3Hex_2$-itol in the eluted fraction (Figure 5D). The two-step fractionation therefore succeeded in isolating the permethylated sulfated *O*-glycans for more definitive MS/MS sequencing without contribution of ions from isobaric nonsulfated structures.

Curiously and contrary to expectation, the MS/MS data demonstrated that a significant amount of the *O*-glycans derived from this crude preparation of the mouse secondary lymph node, both sulfated and nonsulfated, was terminated with a HexNAc at the nonreducing end instead of placing it proximal to the reducing-end GalNAc as the more commonly encountered Core 3 or 4 structures. While several of the structures could be tentatively assigned as having a terminal Cad/Sd^a epitope, NeuAcα2-3(GalNAcβ1-4)Galβ1-4GlcNAc- (Dohi and Kawamura 2008), others were found lacking the terminal sialic acids (Table II, data not shown). In the case of the sulfated structure represented by the signal at *m/z* 1677 (Figure 5D), the presence of both nonreducing terminal HexNAc and NeuAc is clearly identified by the corresponding Y ions at *m/z* 1418 and 1302, respectively, while the loss of both gave the fragment ion at *m/z* 1043 and a prominent G ion at *m/z* 1009 to support a 3,4-substituted Hex. The next $^{1.5}$X and Y ion pairs at 881/853 and 548/520 resulting from loss of an entire terminal NeuAc-(HexNAc)Hex-motif followed by a sulfated HexNAc residue firmly establish the NeuAc-(HexNAc)Hex-(SO_3)HexNAc- sequence. The same Core 2 structure without the sulfate moiety was similarly assigned and attributed to the $[M+Na]^+$ signal at *m/z* 1589 (MS/MS data not shown) found in the unbound fraction (Figure 5A). While full characterization of the implicated structures awaits further chemical analyses, the findings do underline the importance of facilitated MS/MS in revealing structural novelty that would not have been possible by MS mapping alone.

Discussion

Earlier work based on FAB-MS analysis (Dell et al. 1991; Siciliano et al. 1993) has shown that sulfated *N*-glycans could indeed be permethylated using a modified Hakomori methylation procedure (Hakomori 1964) but tedious and technically demanding in preparing the requisite methylsulfinyl carbanion. For most other routine work involving permethylation of nonsulfated glycans, the NaOH/DMSO slurry method first introduced by Ciucanu and Kerek (1984) is most commonly used since it is much simpler to be performed by most laboratories (Dell et al. 1994; Wada et al. 2007). Its successful application to sulfated glycans was nonetheless a moot point until recently. We are in fact the first to show that a mapping of the sulfated glycome from tissues such as the mouse lymph node can be achieved by MALDI-MS analysis of the NaOH permethylated sample in the negative-ion mode (Mitoma et al. 2007). The critical step is to avoid the conventional partitioning against organic solvent such as chloroform after the permethylation reaction since a substantial amount of the negatively charged sulfated glycans,

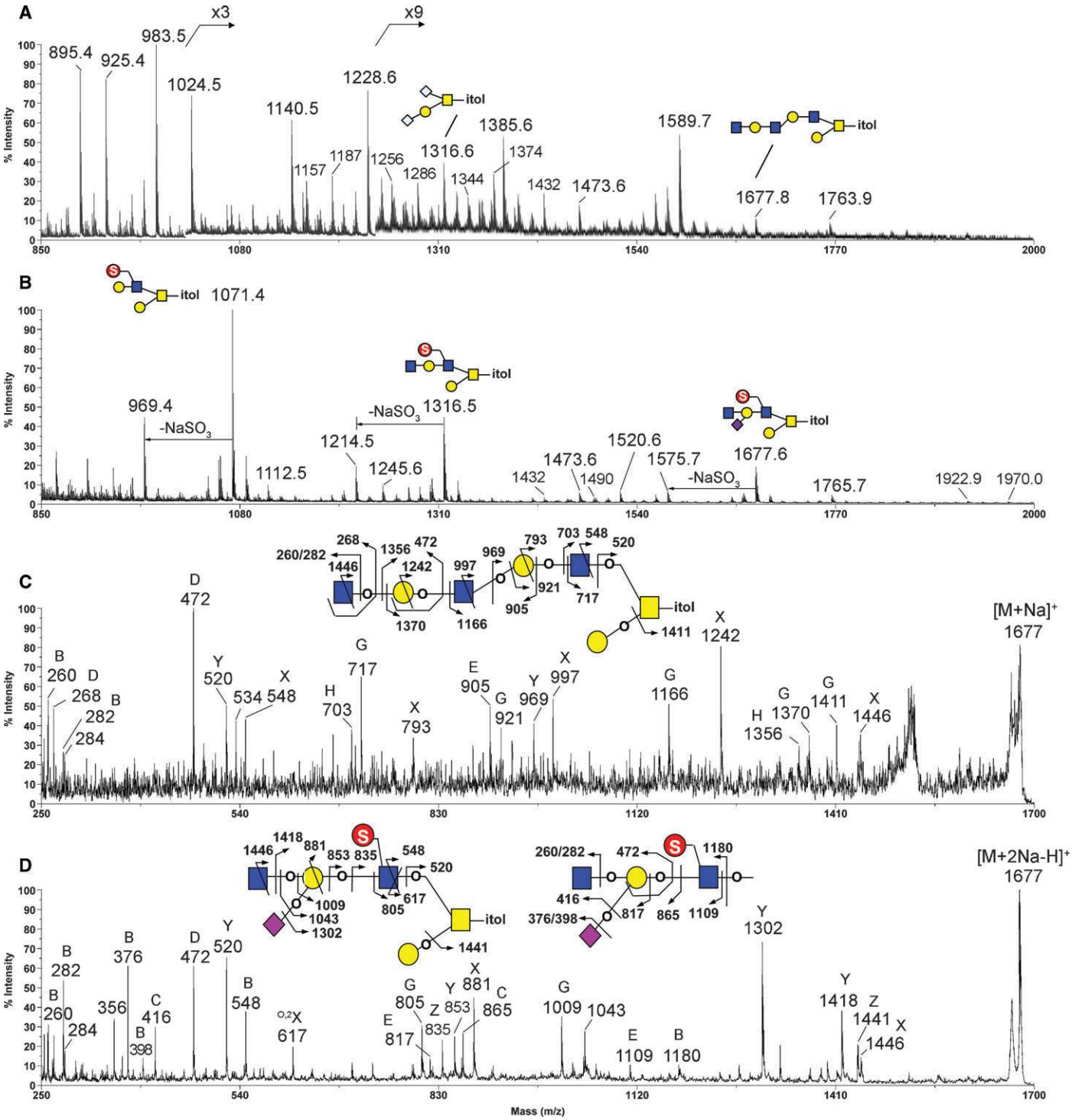

Fig. 5. MALDI-MS profiles and MS/MS analysis of permethylated *O*-glycans from mice secondary lymph nodes in the positive-ion mode. The 25% acetonitrile fraction from C18 Sep-Pak was further fractionated on NH_2-beads, resulting in the unbound (**A**) and ammonium acetate eluted (**B**) fractions containing nonsulfated and sulfated *O*-glycans, respectively (see Table II for a compiled list of assigned molecular ion signals). Loss of sodium sulfite from the molecular ions to give signals at 102 u lower was commonly observed for the sulfated glycans in (**B**). Each of the prominent signals in (**B**) was subjected to MS/MS analysis and the deduced sulfated *O*-glycan structures are as annotated. For the two signals at *m/z* 1316 and 1677 that were also detected in the unbound fraction, additional MS/MS was performed to ascertain their corresponding structures. The MS/MS spectra for the signal at *m/z* 1677 as found in the unbound and eluted fractions are shown in (**C**) and (**D**), respectively.

especially those of smaller size and/or multiply sulfated, will be lost into the aqueous layer. A passing through C18 SPE is sufficient to clean-up the sample from the reagents for MS analysis, as well as to effect a crude separation, as demonstrated previously and more thoroughly investigated here.

The solution-based NaOH/DMSO methylation procedure has recently been adapted by others to solid-phase methylation with NaOH beads packed into the spin column and sample in DMSO/CH_3I recycled through several times by low speed centrifugation (Kang et al. 2008). While gaining in speed and convenience, the efficiency of this method in permethylating sulfated glycans has not yet been fully demonstrated against more complicated glycomic samples other than the nonsialylated, sulfated biantennary *N*-glycans derived from a standard bovine thyroid stimulating hormone (Lei et al. 2009). We have noted instead that better permethylation of sialylated sulfated glycans was achieved with prolonged reaction time conducted at low temperature using the conventional method of applying NaOH/DMSO slurry to dried sample followed by the addition of methyl iodide. Bearing these in mind, the reaction is surprisingly robust and can be readily performed by most laboratories already familiar with the permethylation technique. It was further noted that, under the same reaction conditions, the phosphate group on glycan would be mono- or di-*O*-methylesterified, as also noted by others previously (McConville et al. 1990), whereas the sulfates would not. Although the phosphorylated high mannose glycan structure has not been previously reported for this sample source, we have further confirmed its identity by virtue of its susceptibility to alkaline phosphatase digestion and MS/MS analysis (data not shown). The permethylation procedure therefore provides an easy way of differentiating sulfate from phosphate substituent, which is similar in nominal mass increment, by MS analysis alone.

The experimental workflow for analyzing sulfoglycomics we have now developed is shown in Figure 6. Sulfated glycans and sulfated sialylated glycans can be permethylated efficiently using the optimized NaOH permethylation method in conjunction with post-derivatization clean-up and fractionation using C18 reverse-phase SPE cartridge and microtip self-packed with NH_2-beads. The resulting fractions can be analyzed in both positive- and negative-ion modes and, importantly, be each subjected to high energy CID-MS/MS on a MALDI TOF/TOF to enable highly informative sequencing in the positive-ion mode. It is anticipated that the permethyl derivatives will be equally useful for an alternative analytical platform such as one that employs multistage activation MS^n strategy based on advanced ion trap instruments (Ashline et al. 2005, 2007; Lapadula et al. 2005; Zhang et al. 2005). An important observation is that under both low and high energy CID MS/MS, the sulfated moiety is relatively stable. Thus, glycosidic cleavages, as well as the cross ring cleavages and concerted double cleavages, which are essential for linkage-specific sequencing can occur in a fashion similar to those afforded by nonsulfated glycans. Our work demonstrated that what was established as the characteristic fragmentation pattern for the permethylated nonsulfated glycans can be readily applied to the sulfated glycans, the sequencing of which therefore does not impose a further level of complexity. Where needed, the isolated permethylated sulfated glycan fraction can be further subjected to chemical methanolysis to selectively replace the sulfate with the free hydroxy group, as have been employed for earlier less sensitive FAB-MS analysis (Khoo et al. 1993; Taguchi et al. 1996) to assist MS-mapping and localization of sulfate moiety in the positive-ion mode. This strategy has also been recently re-introduced with an additional re-perdeuteromethylation step after methanolysis to tag the sulfate with CD_3 (Lei et al. 2009). Either way is possible but both have to deal with incomplete desulfation and possible desialylation, as well as incomplete methylation in the first place. The ability to isolate the fully permethylated sulfated glycans for direct MS/MS analysis therefore constitutes a desirable step prior to further chemical manipulation.

The challenge, as usual then, is more on resolving the isobaric and isomeric structures typically present in a glycome, namely to be able to detect at the MS level as many resolved peaks as possible at high sensitivity. It should be noted that application of NH_2-based charge fractionation and other forms of anion-exchange chromatography on native glycans is a common practice in glycan analysis to isolate the sulfated glycans away from the dominating neutral ones (Green and Baenziger 1986; Mawhinney et al. 1987; Pfeiffer et al. 1989; Kawashima et al. 2005). The usual problem, however, is that the highly abundant sialylated but nonsulfated structures will be coisolated unless the carboxylic groups are first neutralized by chemical derivatization (Karlsson et al. 1995; Powell and Harvey 1996; Miura et al. 2007). Application of this fractionation step on the permethyl derivatives, as demonstrated here, is therefore more selective. Recently, an alternative strategy has been developed in which nonderivatized sulfated glycans were shown to be eluting earlier than sialylated glycans on an open column packed with strong cation-exchange resin (Garenaux et al. 2008). Success was, however, demonstrated only at the level of a relatively large sample preparation scale, whereas our current fractionation scheme has been developed for microscale applications.

More advances in sample fractionation and handling can be anticipated, which should collectively enable the MS analysis of sulfated glycome at a sensitivity level conducive to addressing important glycobiology questions. This would be more informative than what are now mostly inferred from immunostaining using a panel of monoclonal antibodies, which normally preclude identification of unanticipated epitopes and the underlying glycan carriers. The application of MS-based sulfoglycomics for tissues and cells is still at its infancy. In comparison with the multidimensional HPLC mapping of the sulfated *N*-glycans tagged with fluorescent probe (Yagi et al. 2005), the MS approach has the added strengths in being equally applicable to reduced *O*-glycans and better poised to identify novel sulfated epitopes in an unbiased discovery mode, as demonstrated in this work. Among the many other *O*-glycans from the mouse lymph node found to carry an extra terminal HexNAc, the ones with both terminal HexNAc and NeuAc substituents on a 3,4-branched Hex cannot be simply interpreted as incomplete galactosylation of a LacNAc unit. Even for those without accompanying NeuAc, our MS/MS data indicated that the terminal HexNAc is 4-linked to the Hex and not 3-linked. To our knowledge, a sulfated Sd^a epitope or one with an overall sequence of NeuAc-(HexNAc)Hex-(SO_3)HexNAc has not been previously reported. It serves to illustrate what an MS-based sulfoglycomics can deliver although more following up analyses are obviously needed to further validate its stereochemistry and tissue/cell-type specificity. This is a timely and urgently needed development in view of sulfated terminal epitopes other than sulfo- sialyl Le^x or sulfated glycosaminoglycan units being increasingly implicated as

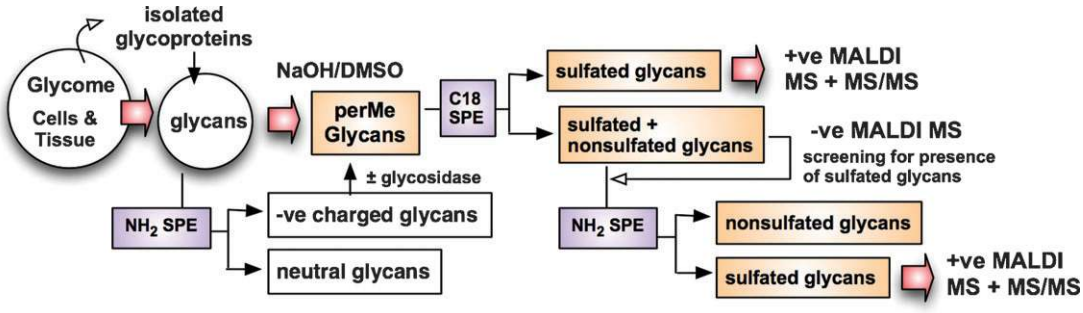

Fig. 6. A proposed experimental workflow for sulfoglycomics. The pipeline established in this work is geared toward obtaining permethylated sulfated glycans for initial high sensitivity MS screening in the negative-ion mode and subsequent MS/MS analysis in the positive-ion mode after further fractionation to enable detection in the positive-ion mode. Although MALDI-based MS was described in this work, the permethylated sample is equally amenable for ESI-based MS analysis. The NH_2-based fractionation can also be applied to nonpermethylated glycans if need arises to isolate them for exoglycosidase digestions and/or other manipulations that can only be effected at the level of native glycans.

the preferred high affinity ligands of galectins and Siglecs alike through glycan array studies (Bochner et al. 2005; Carlsson et al. 2007).

Material and methods

Glycan standards

A tetrasulfated diLacNAc tetrasaccharide [6′,6-HSO_3^--GalGlcNAc]$_2$ standard was derived from shark cartilage keratan sulfate by enzymatic hydrolysis with keratanase II (Kubota et al. 2000). Partial desulfation of the tetrasulfated diLacNAc was performed by adding 0.5 N anhydrous methanolic hydrochloric acid (MeOH-HCl, Supelco, Bellefonte, PA) and left at room temperature for 30 min. *N*-Glycans were released from tryptic peptides of recombinant erythropoietin expressed in BHK21 cells (Advanced Gene Technology Corp, Taiwan) by PNGase F using a standard protocol as described previously (Dell et al. 1994). Sulfated *O*-glycans were released along with the nonsulfated ones from human ovarian cyst sample #350 (HOC350) as described previously (Wu et al. 2007).

Secondary lymph nodes

Peripheral, mesenteric lymph nodes, and peyer's patches from one mice were sliced and squeezed in the 0.1 M NH_4HCO_3 buffer, boiled for 10 min, and lyophilized. The lyophilized samples were first subjected to MeOH/chloroform (1:2) delipidation, pelleted down by centrifugation at 2000 × *g*, and then extracted by 6 M guanidine chloride in 50 mM Tris-HCl with 1 mM $CaCl_2$, pH 8.4, at 4°C. Extracted proteins were reduced by 20 mM dithiothreitol (Sigma) in 6 M guanidine chloride at 37°C for 4 h, followed by alkylation with 50 mM iodoacetamide (Sigma) at room temperature in the dark for another 4 h, and then dialyzed against ddH_2O. The dialyzed samples were digested with trypsin and chymotrypsin (Sigma), each for 4 h, in the 50 mM ammonium bicarbonate buffer, pH 8, at 37°C, followed by overnight treatment with PNGase F (Roche). Released *N*-glycans were isolated from the peptides by passing through C18 Sep-Pak cartridge (Waters) in 5% acetic acid. Retained peptides were then eluted with 20–60% propanol/5% acetic acid and used for subsequent release of *O*-glycans by reductive elimination (1 M $NaBH_4$/0.05 N NaOH, 37°C, 3 days). After terminating the chemical reaction by pure acetic acid on ice, the solution was taken through Dowex 50 × 8 column (H^+ form, Bio-Rad) in 5% acetic acid, dried, and coevaporated with 10% acetic acid in methanol to remove borates.

Permethylation of sulfated glycans

Glycan sample dried down in the glass tube was redissolved in a slurry of finely ground NaOH pellets in dimethyl sulfoxide (~0.2 mL), followed by the addition of 0.1 mL of methyl iodide. The reaction mixture was gently vortexed for 3 h at 4°C and then quenched on ice with 0.2 mL of cold water, followed by careful neutralization with 30% aqueous acetic acid, and then applied directly to a pre-washed and equilibrated C18 Sep-Pak cartridge (Waters). Hydrophilic salts and contaminants were step-wise washed off with 5 mL of water, 2.5% and 10% acetonitrile. Subsequently, permethylated disulfated *N*-linked glycans were eluted with 5 mL of 25% acetonitrile, whereas the monosulfated *N*-glycans could be found in both the 25% and the next 5 mL of 50% acetonitrile fractions. Nonsulfated glycans were collected in the 50% acetonitrile fraction, as well as later eluting 75–100% acetonitrile fraction for larger ones. Under similar conditions, both the sulfated and nonsulfated smaller *O*-glycans were eluted in earlier fractions. For further sample clean-up or concentration, when necessary, the permethyl derivatives were dissolved in 20 μL of 10% acetonitrile and taken up by pre-washed $ZipTip_{C18}$ (Millipore). After washing several times with 0.1% trifluoroacetic acid, the sulfated glycans were eluted by 10 μL of 50% acetonitrile/0.1% trifluoroacetic acid, or less volume, for collection into microtubes or direct spotting onto the MALDI target plate.

Fractionation by amine column

Amine beads (Nucleosil, 5 μm particle size, 100% pore size) were packed into pipette tip with the tapered end plugged by a filter paper. Depending on sample quantity, the volume of packed beads can range from as little as 0.5 μL to about 5 μL, using microtips of different sizes and different wash/elution volumes (50–200 μL). The packed amine micro-column was first conditioned and washed sequentially with 5% acetonitrile/0.1% formic acid, 50% acetonitrile/0.1% formic acid, and 95% acetonitrile/0.1% formic acid. The native glycan sample was dissolved in 95% acetonitrile for loading, and hydrophobic contaminants were washed off with the same solvent. Neutral glycans were then eluted with 5% acetonitrile, monosulfated or

monosialylated glycans with 5% acetonitrile/0.1% formic acid (pH ~ 2.5), and multiply negatively charged glycans such as disulfated glycans, monosialylated monosulfated glycans, or multisialylated glycans with 5% acetonitrile/0.25% trifluoroacetic acid (pH ~ 1.5). Using the same pre-conditioned amine beads-packed micro-column, sulfated and nonsulfated permethylated glycans can likewise be fractionated. Permethylated sample was dissolved in 100% acetonitrile for loading. Nonsulfated permethylated glycans such as the neutral and sialylated ones were collected in the unbound fraction and an additional 95% acetonitrile wash fraction. Mono- and disulfated permethylated glycans were eluted with 2.5 mM and 10 mM ammonium acetate in 50% acetonitrile, respectively.

MALDI-MS and MS/MS analyses

MALDI-MS and MS/MS analyses of permethylated glycans were performed on 4700 Proteomics Analyzer (Applied Biosystems, Framingham, MA), operated in the reflectron mode. For MS acquisition, the permethylated samples in acetonitrile were mixed 1:1 with 2,5-dihydroxybenzoic acid (DHB) matrix (10 mg/mL in 50% acetonitrile) or 1:1 with 3,4-diaminobenzophenone (DABP) matrix (Fu et al. 2006; Xu et al. 2006) (10 mg/mL in 75% acetonitrile/0.1% trifluoroacetic acid) (Acros Organics, NJ) for spotting onto the target plate for both positive- and negative-ion mode analyses. The potential difference between the source acceleration voltage and the collision cell was set at 3 kV to obtain the desirable high energy CID fragmentation pattern. Other parameters and conditions were exactly as described before (Yu et al. 2006).

Funding

Taiwan National Science Council NRPGM grant (NSC-96-3112-B-001-018; NSC-97-3112-B-001-018) to the Core Facilities for Proteomics and Glycomics and an Academia Sinica Program grant (AS-97-FP-L04 to KHK).

Conflict of interest statement

None declared.

Abbreviations

CID, collision-induced dissociation; DMSO, dimethyl sulfoxide; ESI, electrospray ionization; FAB, fast-atom-bombardment; MALDI, matrix-assisted laser desorption/ionization; MS, mass spectrometry; Q/TOF, quadrupole/time-of-flight; LacNAc, *N*-acetyllactosamine; OMe, *O*-methyl substituent or methoxy; SPE, solid phase extraction.

References

Alon R, Rosen S. 2007. Rolling on *N*-linked glycans: A new way to present L-selectin binding sites. *Nat Immunol*. 8:339–341.

Ashline D, Singh S, Hanneman A, Reinhold V. 2005. Congruent strategies for carbohydrate sequencing: 1. Mining structural details by MS^n. *Anal Chem*. 77:6250–6262.

Ashline DJ, Lapadula AJ, Liu YH, Lin M, Grace M, Pramanik B, Reinhold VN. 2007. Carbohydrate structural isomers analyzed by sequential mass spectrometry. *Anal Chem*. 79:3830–3842.

Barboza M, Duschak VG, Fukuyama Y, Nonami H, Erra-Balsells R, Cazzulo JJ, Couto AS. 2005. Structural analysis of the *N*-glycans of the major cysteine proteinase of *Trypanosoma cruzi*. Identification of sulfated high-mannose type oligosaccharides. *FEBS J*. 272:3803–3815.

Bochner BS, Alvarez RA, Mehta P, Bovin NV, Blixt O, White JR, Schnaar RL. 2005. Glycan array screening reveals a candidate ligand for Siglec-8. *J Biol Chem*. 280:4307–4312.

Capon C, Maes E, Michalski JC, Leffler H, Kim YS. 2001. Sd(a)-antigen-like structures carried on core 3 are prominent features of glycans from the mucin of normal human descending colon. *Biochem J*. 358:657–664.

Capon C, Wieruszeski JM, Lemoine J, Byrd JC, Leffler H, Kim YS. 1997. Sulfated lewis X determinants as a major structural motif in glycans from LS174T-HM7 human colon carcinoma mucin. *J Biol Chem*. 272:31957–31968.

Carlsson S, Oberg CT, Carlsson MC, Sundin A, Nilsson UJ, Smith D, Cummings RD, Almkvist J, Karlsson A, Leffler H. 2007. Affinity of galectin-8 and its carbohydrate recognition domains for ligands in solution and at the cell surface. *Glycobiology*. 17:663–676.

Chen HS, Chen JM, Lin CW, Khoo KH, Tsai IH. 2008. New insights into the functions and *N*-glycan structures of factor X activator from Russell's viper venom. *FEBS J*. 275:3944–3958.

Ciucanu I, Kerek F. 1984. A simple and rapid method for the permethylation of carbohydrates. *Carbohydr Res*. 131:209–217.

Degroote S, Ducourouble MP, Roussel P, Lamblin G. 1999. Sequential biosynthesis of sulfated and/or sialylated Lewis x determinants by transferases of the human bronchial mucosa. *Glycobiology*. 9:1199–1211.

Dell A, Morris HR, Greer F, Redfern JM, Rogers ME, Weisshaar G, Hiyama J, Renwick AG. 1991. Fast-atom-bombardment mass spectrometry of sulphated oligosaccharides from ovine lutropin. *Carbohydr Res*. 209:33–50.

Dell A, Reason AJ, Khoo KH, Panico M, McDowell RA, Morris HR. 1994. Mass spectrometry of carbohydrate-containing biopolymers. *Methods Enzymol*. 230:108–132.

Dohi T, Kawamura YI. 2008. Incomplete synthesis of the Sda/Cad blood group carbohydrate in gastrointestinal cancer. *Biochim Biophys Acta*. 1780:467–471.

Fu Y, Xu S, Pan C, Ye M, Zou H, Guo B. 2006. A matrix of 3,4-diaminobenzophenone for the analysis of oligonucleotides by matrix-assisted laser desorption/ionization time-of-flight mass spectrometry. *Nucleic Acids Res*. 34:e94.

Fukuda M, Hiraoka N, Akama TO, Fukuda MN. 2001. Carbohydrate-modifying sulfotransferases: Structure, function, and pathophysiology. *J Biol Chem*. 276:47747–47750.

Gallego RG, Blanco JL, Thijssen-van Zuylen CW, Gotfredsen CH, Voshol H, Duus JO, Schachner M, Vliegenthart JF. 2001. Epitope diversity of *N*-glycans from bovine peripheral myelin glycoprotein P0 revealed by mass spectrometry and nano probe magic angle spinning 1H NMR spectroscopy. *J Biol Chem*. 276:30834–30844.

Garenaux E, Yu SY, Florea D, Strecker G, Khoo KH, Guerardel Y. 2008. A single step method for purification of sulfated oligosaccharides. *Glycoconj J*. 25:903–915.

Geyer H, Geyer R. 2006. Strategies for analysis of glycoprotein glycosylation. *Biochim Biophys Acta*. 1764:1853–1869.

Green ED, Baenziger JU. 1986. Separation of anionic oligosaccharides by high-performance liquid chromatography. *Anal Biochem*. 158:42–49.

Green ED, Baenziger JU. 1988. Asparagine-linked oligosaccharides on lutropin, follitropin, and thyrotropin: I. Structural elucidation of the sulfated and sialylated oligosaccharides on bovine, ovine, and human pituitary glycoprotein hormones. *J Biol Chem*. 263:25–35.

Hakomori S. 1964. A rapid permethylation of glycolipid, and polysaccharide catalyzed by methylsulfinyl carbanion in dimethyl sulfoxide. *J Biochem*. 55:205–208.

Harvey DJ, Bateman RH, Green MR. 1997. High-energy collision-induced fragmentation of complex oligosaccharides ionized by matrix-assisted laser desorption/ionization mass spectrometry. *J Mass Spectrom*. 32:167–187.

Haslam SM, North SJ, Dell A. 2006. Mass spectrometric analysis of *N*- and *O*-glycosylation of tissues and cells. *Curr Opin Struct Biol*. 16:584–591.

Hemmerich S, Rosen SD. 2000. Carbohydrate sulfotransferases in lymphocyte homing. *Glycobiology*. 10:849–856.

Hernandez Mir G, Helin J, Skarp KP, Cummings RD, Makitie A, Renkonen R, Leppanen A. 2009. Glycoforms of human endothelial CD34 that bind L-selectin carry sulfated sialyl Lewis x capped *O*- and *N*-glycans. *Blood*. 14:733–741.

Hitchcock AM, Yates KE, Costello CE, Zaia J. 2008. Comparative glycomics of connective tissue glycosaminoglycans. *Proteomics*. 8:1384–1397.

Hooper LV, Manzella SM, Baenziger JU. 1996. From legumes to leukocytes: Biological roles for sulfated carbohydrates. *FASEB J*. 10:1137–1146.

Hortin G, Green ED, Baenziger JU, Strauss AW. 1986. Sulphation of proteins secreted by a human hepatoma-derived cell line. Sulphation of *N*-linked oligosaccharides on alpha 2HS-glycoprotein. *Biochem J*. 235:407–414.

Jang-Lee J, North SJ, Sutton-Smith M, Goldberg D, Panico M, Morris H, Haslam S, Dell A. 2006. Glycomic profiling of cells and tissues by mass spectrometry: Fingerprinting and sequencing methodologies. *Methods Enzymol*. 415:59–86.

Kanda H, Tanaka T, Matsumoto M, Umemoto E, Ebisuno Y, Kinoshita M, Noda M, Kannagi R, Hirata T, Murai T, et al. 2004. Endomucin, a sialomucin expressed in high endothelial venules, supports L-selectin-mediated rolling. *Int Immunol*. 16:1265–1274.

Kang P, Mechref Y, Novotny MV. 2008. High-throughput solid-phase permethylation of glycans prior to mass spectrometry. *Rapid Commun Mass Spectrom*. 22:721–734.

Karlsson NG, Karlsson H, Hansson GC. 1995. Strategy for the investigation of *O*-linked oligosaccharides from mucins based on the separation into neutral, sialic acid- and sulfate-containing species. *Glycoconj J*. 12:69–76.

Karlsson NG, Karlsson H, Hansson GC. 1996. Sulphated mucin oligosaccharides from porcine small intestine analysed by four-sector tandem mass spectrometry. *J Mass Spectrom*. 31:560–572.

Kawasaki N, Haishima Y, Ohta M, Itoh S, Hyuga M, Hyuga S, Hayakawa T. 2001. Structural analysis of sulfated *N*-linked oligosaccharides in erythropoietin. *Glycobiology*. 11:1043–1049.

Kawashima H. 2006. Roles of sulfated glycans in lymphocyte homing. *Biol Pharm Bull*. 29:2343–2349.

Kawashima H, Petryniak B, Hiraoka N, Mitoma J, Huckaby V, Nakayama J, Uchimura K, Kadomatsu K, Muramatsu T, Lowe JB, et al. 2005. *N*-Acetylglucosamine-6-*O*-sulfotransferases 1 and 2 cooperatively control lymphocyte homing through L-selectin ligand biosynthesis in high endothelial venules. *Nat Immunol*. 6:1096–1104.

Khoo KH, Morris HR, McDowell RA, Dell A, Maccarana M, Lindahl U. 1993. FABMS/derivatisation strategies for the analysis of heparin-derived oligosaccharides. *Carbohydr Res*. 244:205–223.

Kubota M, Yoshida K, Tawada A, Ohashi M. 2000. Characterization of oligosaccharides of the lactosamin sulfates by tandem mass spectrometry. *Eur J Mass Spectrom*. 6:193–203.

Lapadula AJ, Hatcher PJ, Hanneman AJ, Ashline DJ, Zhang H, Reinhold VN. 2005. Congruent strategies for carbohydrate sequencing: 3. OSCAR: An algorithm for assigning oligosaccharide topology from MS^n data. *Anal Chem*. 77:6271–6279.

Lei M, Mechref Y, Novotny MV. 2009. Structural analysis of sulfated glycans by sequential double-permethylation using methyl iodide and deuteromethyl iodide. *J Am Soc Mass Spectrom*.

Lemoine J, Fournet B, Despeyroux D, Jennings KR, Rosenberg R, de Hoffmann E. 1993. Collision-induced dissociation of alkali metal cationized and permethylated oligosaccharides: Influence of the collision energy and of the collision gas for the assignment of linkage position. *J Am Soc Mass Spectrom*. 4:197–203.

Liedtke S, Geyer H, Wuhrer M, Geyer R, Frank G, Gerardy-Schahn R, Zahringer U, Schachner M. 2001. Characterization of *N*-glycans from mouse brain neural cell adhesion molecule. *Glycobiology*. 11:373–384.

Lo-Guidice JM, Wieruszeski JM, Lemoine J, Verbert A, Roussel P, Lamblin G. 1994. Sialylation and sulfation of the carbohydrate chains in respiratory mucins from a patient with cystic fibrosis. *J Biol Chem*. 269:18794–18813.

Mawhinney TP, Adelstein E, Gayer DA, Landrum DC, Barbero GJ. 1992. Structural analysis of monosulfated side-chain oligosaccharides isolated from human tracheobronchial mucous glycoproteins. *Carbohydr Res*. 223:187–207.

Mawhinney TP, Adelstein E, Morris DA, Mawhinney AM, Barbero GJ. 1987. Structure determination of five sulfated oligosaccharides derived from tracheobronchial mucus glycoproteins. *J Biol Chem*. 262:2994–3001.

McConville MJ, Thomas-Oates JE, Ferguson MA, Homans SW. 1990. Structure of the lipophosphoglycan from *Leishmania* major. *J Biol Chem*. 265:19611–19623.

McEver RP. 2005. A sulfated address for lymphocyte homing. *Nat Immunol*. 6:1067–1069.

Mitoma J, Bao X, Petryanik B, Schaerli P, Gauguet JM, Yu SY, Kawashima H, Saito H, Ohtsubo K, Marth JD, et al. 2007. Critical functions of *N*-glycans in L-selectin-mediated lymphocyte homing and recruitment. *Nat Immunol*. 8:409–418.

Miura Y, Shinohara Y, Furukawa JI, Nagahori N, Nishimura SI. 2007. Rapid and simple solid-phase esterification of sialic acid residues for quantitative glycomics by mass spectrometry. *Chem—A Eur J*. 13:4797–4804.

Morelle W, Canis K, Chirat F, Faid V, Michalski JC. 2006. The use of mass spectrometry for the proteomic analysis of glycosylation. *Proteomics*. 6:3993–4015.

Morelle W, Slomianny MC, Diemer H, Schaeffer C, van Dorsselaer A, Michalski JC. 2004. Fragmentation characteristics of permethylated oligosaccharides using a matrix-assisted laser desorption/ionization two-stage time-of-flight (TOF/TOF) tandem mass spectrometer. *Rapid Commun Mass Spectrom.*, 18:2637–2649.

Murakami T, Natsuka S, Nakakita S, Hase S. 2007. Structure determination of a sulfated *N*-glycans, candidate for a precursor of the selectin ligand in bovine lung. *Glycoconj J*. 24:195–206.

Pfeiffer G, Schmidt M, Strube KH, Geyer R. 1989. Carbohydrate structure of recombinant human uterine tissue plasminogen activator expressed in mouse epithelial cells. *Eur J Biochem*. 186:273–286.

Powell AK, Harvey DJ. 1996. Stabilization of sialic acids in *N*-linked oligosaccharides and gangliosides for analysis by positive ion matrix-assisted laser desorption/ionization mass spectrometry. *Rapid Commun Mass Spectrom*. 10:1027–1032.

Robbe C, Capon C, Coddeville B, Michalski JC. 2004. Diagnostic ions for the rapid analysis by nano-electrospray ionization quadrupole time-of-flight mass spectrometry of *O*-glycans from human mucins. *Rapid Commun Mass Spectrom*. 18:412–420.

Satomaa T, Renkonen O, Helin J, Kirveskari J, Makitie A, Renkonen R. 2002. *O*-Glycans on human high endothelial CD34 putatively participating in L-selectin recognition. *Blood*. 99:2609–2611.

Siciliano RA, Morris HR, McDowell RA, Azadi P, Rogers ME, Bennett HP, Dell A. 1993. The Lewis x epitope is a major non-reducing structure in the sulphated *N*-glycans attached to Asn-65 of bovine pro-opiomelanocortin. *Glycobiology*. 3:225–239.

Spina E, Sturiale L, Romeo D, Impallomeni G, Garozzo D, Waidelich D, Glueckmann M. 2004. New fragmentation mechanisms in matrix-assisted laser desorption/ionization time-of-flight/time-of-flight tandem mass spectrometry of carbohydrates. *Rapid Commun Mass Spectrom*. 18:392–398.

Stephens E, Maslen SL, Green LG, Williams DH. 2004. Fragmentation characteristics of neutral *N*-linked glycans using a MALDI-TOF/TOF tandem mass spectrometer. *Anal Chem*. 76:2343–2354.

Suzuki N, Su TH, Wu SW, Yamamoto K, Khoo KH, Lee YC. 2009. Structural analysis of *N*-glycans from gull egg white glycoproteins and egg yolk IgG. *Glycobiology*. 19:693–706.

Taguchi T, Iwasaki M, Muto Y, Kitajima K, Inoue S, Khoo KH, Morris HR, Dell A, Inoue Y. 1996. Occurrence and structural analysis of highly sulfated multiantennary *N*-linked glycan chains derived from a fertilization-associated carbohydrate-rich glycoprotein in unfertilized eggs of *Tribolodon hakonensis*. *Eur J Biochem*. 238:357–367.

Thomsson KA, Karlsson H, Hansson GC. 2000. Sequencing of sulfated oligosaccharides from mucins by liquid chromatography and electrospray ionization tandem mass spectrometry. *Anal Chem*. 72:4543–4549.

Thomsson KA, Karlsson NG, Hansson GC. 1999. Liquid chromatography-electrospray mass spectrometry as a tool for the analysis of sulfated oligosaccharides from mucin glycoproteins. *J Chromatogr A*. 854:131–139.

Thomsson KA, Schulz BL, Packer NH, Karlsson NG. 2005. MUC5B glycosylation in human saliva reflects blood group and secretor status. *Glycobiology*. 15:791–804.

Wada Y, Azadi P, Costello CE, Dell A, Dwek RA, Geyer H, Geyer R, Kakehi K, Karlsson NG, Kato K, et al. 2007. Comparison of the methods for profiling glycoprotein glycans—HUPO Human Disease Glycomics/Proteome Initiative multi-institutional study. *Glycobiology*. 17:411–422.

Wu AM, Khoo KH, Yu SY, Yang ZG, Kannagi R, Watkins WM. 2007. Glycomic mapping of pseudomucinous human ovarian cyst glycoproteins: Identification of Lewis and sialyl Lewis glycotopes. *Proteomics*. 7:3699–3717.

Wuhrer M, Catalina MI, Deelder AM, Hokke CH. 2007. Glycoproteomics based on tandem mass spectrometry of glycopeptides. *J Chromatogr B Analyt Technol Biomed Life Sci*. 849:115–128.

Xu S, Ye M, Xu D, Li X, Pan C, Zou H. 2006. Matrix with high salt tolerance for the analysis of peptide and protein samples by desorption/ionization time-of-flight mass spectrometry. *Anal Chem*. 78:2593–2599.

Yagi H, Takahashi N, Yamaguchi Y, Kimura N, Uchimura K, Kannagi R, Kato K. 2005. Development of structural analysis of sulfated *N*-glycans by multidimensional high performance liquid chromatography mapping methods. *Glycobiology*. 15:1051–1060.

Yu SY, Khoo KH, Yang Z, Herp A, Wu AM. 2008. Glycomic mapping of *O*- and *N*-linked glycans from major rat sublingual mucin. *Glycoconj J*. 25:199–212.

Yu SY, Wu SW, Khoo KH. 2006. Distinctive characteristics of MALDI-Q/TOF and TOF/TOF tandem mass spectrometry for sequencing of permethylated complex type *N*-glycans. *Glycoconj J*. 23:355–369.

Zaia J. 2008. Mass spectrometry and the emerging field of glycomics. *Chem Biol*. 15:881–892.

Zaia J. 2009. On-line separations combined with MS for analysis of glycosaminoglycans. *Mass Spectrometry Reviews*. 28:254–272.

Zhang H, Singh S, Reinhold VN. 2005. Congruent strategies for carbohydrate sequencing: 2. FragLib: An MS^n spectral library. *Anal Chem*. 77:6263–6270.